PARTICLE COUNTING BY FLUORESCENCE CORRELATION SPECTROSCOPY

Simultaneous Measurement of Aggregation and Diffusion of Molecules in Solutions and in Membranes

TOBIAS MEYER AND HANSGEORG SCHINDLER
Department of Biophysical Chemistry, Biocenter of the University of Basel, 4056 Basel, Switzerland

ABSTRACT A method for simultaneous determination of molar weights (M) and lateral diffusion constants (D) of particles in three- and two-dimensional systems is described. Spontaneous concentration fluctuations in space and time are analyzed, by monitoring fluctuations in the fluorescence from fluorescein-labeled molecules (1 dye/molecule is sufficient), excited by a rotating laser spot. For particles in solution, M values are determined over the range of 3×10^2 to 3×10^{11} daltons, and D values can be determined from $\sim 10^{-7}$ to 10^{-10} cm^2/s. The time for a determination is ~ 1 min. Aggregation can be followed by changes of either M or D. This method is used to study the calcium dependence of vesicle aggregation or fusion, and the time course of aggregate formation of porin (an *Escherichia Coli* outer membrane protein) in lipid monolayers. Essential parameters for the development of the method are described. Equations to estimate the signal-to-noise ratios and to find the optimal free parameters for a specific application are derived. The theoretical predictions for the correlation function of the signal and for the signal-to-noise ratio are compared with observed values.

INTRODUCTION

Fluorescent markers have been widely used to assess organization and transport properties of biomolecules both in isolation and in their natural context. Fluorescence spectroscopy, applied to biological and model membranes, has been particularly successful in analyzing mobility or lateral diffusion of membrane constituents with a major contribution from the fluorescence recovery after photobleaching (FRAP) technique over the last decade (Peters et al., 1974; Koppel et al., 1976; for technical improvements see Axelrod et al., 1983; for a data review see for example Cherry, 1979). In recent years new techniques have emerged which use instrumentation similar to that used in FRAP, but take advantage of different types of data collection and analysis to obtain information about number density and other properties of labeled molecules in addition to their mobility. The first steps in this direction were the development of fluorescence correlation spectroscopy (FCS) (Elson and Magde, 1974; Magde et al., 1974; Elson and Webb, 1975; Koppel et al., 1976; Icenogle and Elson, 1983; Petersen and Elson, 1986) and of fluctuation spectroscopy (FLUSY) (Weissman et al., 1976). In FCS, time-dependent processes, such as lateral diffusion constants (D) and reaction kinetics, are evaluated from signal fluctuations in time. FLUSY provides, in addition, time-independent information by collecting signals from an ensemble of independent subvolumes yielding average particle density n and molar weight M_p. This technique has been further developed since, and has found some practical applications in biology (e.g., as an immunoassay, Nicoli et al., 1980). The scanning of cell surfaces with a focused laser spot (scanning fluorescence correlation spectroscopy) and the analysis of fluctuations in a video image of the cell surface were both used to monitor the aggregate size of membrane components (Petersen, 1984, 1986*a*, *b*; Gross and Webb, 1986; Palmer and Thompson, 1987*a*). Higher order correlation functions were described to be useful in characterizing aggregate distributions of fluorescent molecules (Palmer and Thompson, 1987*b*).

The extraction of particle density, molecular weight, and diffusion coefficients from a homogeneous sample is the objective of the presented method. A major advantage of the new technique is its possibility to directly count the number of independent particles in a defined volume; hence we refer to it as fluorescence particle counting (FPC). The determination of the number of independent particles can be used to follow aggregation processes in time. While FLUSY made use of a rotating sample to

Present addresses for Drs. Meyer and Schindler, respectively, are: Department of Cell Biology, Sherman Fairchild Center, Stanford University School of Medicine, Stanford, CA 94305; Institute of Biophysics, University of Linz, 4040 Linz, Austria.

obtain information from independent subvolumes, FPC uses a rotating laser beam to scan through the different subvolumes. The method can be considered as an advanced version of FLUSY, in which the sensitivity has been improved by several orders of magnitude, allowing signal analysis both in space and time. The use of a circular beam in FPC increases the amount of available information (diffusion coefficient) as compared to scanning FCS. The possibility for a parallel measurement of changes in aggregation states and diffusion coefficients enables the dynamical characterization of aggregation processes.

It is our intention to present a careful study of the inherent potential of FPC with respect to the type of information obtainable, to the accuracy in data evaluation, and to the range of applications as assessed with model systems.

MATERIALS AND SAMPLES

Materials

BSA was purchased from Boehringer Mannheim Diagnostics, Inc. (Houston, TX), thyroglobulin and aldolase from Pharmacia Fine Chemicals (Piscataway, NJ), fluorescein-isothiocyanate (FITC) from Molecular Probes (Junction City, OR), and green fluorescent latex beads from Polysciences, Inc. (Warrington, PA). Phospholipids were purchased from Avanti Polar Lipids, Inc. (Birmingham, AL). Matrix protein (or MX_3 or porin) from *Escherichia Coli* and the detergent octyl-oligooxyethylene were gifts of Dr. J. P. Rosenbusch (Biocenter, Basel, Switzerland), and *E. Coli* lipopolysaccharide was bought from Sigma Chemical Co. (St Louis, MO).

Lipid Vesicles

1-Palmitoyl-2-oleoyl-phosphatidylcholine (POPC), dioleoyl-phosphatidyl-serine (DOPS), 1-palmitoyl(NBD)-2-lauroyl-phosphatidylcholine (PC-NBD), and soybeam phospholipids were dissolved in $CHCl_3$ and dried in vacuum for 30 min in a rotating round glass flask. Standard buffer was added and the lipid mixtures were sonicated for 20 min with a tip sonicator at 4°C in an N_2 atmosphere. After sonication, vesicles were centrifuged for 10 min at 15,000 *g*, and the supernatant was used for the dilution series. The Ca^{2+}-free buffer had in addition 1 mM EGTA, and the Ca^{2+}-containing buffer had instead 5 mM $CaCl_2$. Vesicles for monolayer experiments were prepared by a similar procedure up to the sonication step. Solubilization of vesicles was achieved by shaking the buffer together with ~100 glass beads (2-mm diam) for about 15 min. The average diameter of these vesicles was ~250 nm compared to ~30 nm for sonicated vesicles (determined by light scattering and FPC analysis).

Labeling of Proteins with FITC

Proteins except matrix protein were incubated at 1 mg/ml for 2 h at room temperature, pH 9, with 50 μg FITC/mg protein. Labeled protein was separated from the free dye on a G25 Sephadex column (by 2-cm diam, 10-cm long). Matrix protein was labeled in the presence of 1% polydisperse octyl-oligooxyethylene at 150 μg FITC/mg protein for 12 h. The incubation mixture was dialyzed for 24 h against the same buffer without FITC (two buffer exchanges). Standard buffers were 100 mM NaCl, 20 mM Tris, pH 7.4. 1 mg/ml *p*-phenylenediamine (Merck & Co., Inc., Rahway, NJ) was added as it was found to reduce fluorescein bleaching by a factor of about five.

Determination of Mass Concentrations

Protein-(FITC-labeled) concentrations were determined using a Bio-Rad microassay (Bio Rad Laboratories, Richmond, CA). As a reference, the unlabeled protein with known extinction coefficient at 280 nm was used in the microassay (Handbook of Biochemistry, 1976). A reproducible accuracy of 5% for the weight concentration of the labeled molecule could then be achieved. The dry weight of latex beads was measured after drying for 2 h under high vacuum. The particle concentration was then determined using the diameter of the beads and their density.

Monolayer Preparation

The monolayer trough was cleaned with chromosulfuric acid before use. Further elimination of surfactants was achieved by a 10–60-min suction from the bath surface while triply distilled water was pumped into the bath at a constant rate (10 ml/min). This suction method also allows a precise definition of the surface level above the objective. By scraping a few microliters of the 10 mg/ml vesicle solution onto a wet rough glass slide in contact with the surface of the trough, a high surface pressure forms immediately when native soybean phospholipids are used and more slowly with dimystrioylphosphatidylcholine (DMPC) vesicles.

METHODS

Basic Principle

The number of particles (N) in given subvolumes (V) vary in space, $N_i(r)$, and fluctuate in time, $N_r(t)$, around a common mean $\overline{N_i(r)} = \langle N_r(t) \rangle = N$ (the bar denotes an average in space at time t and $\langle\ \rangle$ denotes an average in time at a defined place denoted by vector $\mathbf{r}$; subvolumes V have the same size). These two types of fluctuations carry different kinds of information. Their simultaneous measurement was the rationale for the technique presented. For this it is required (*a*) to monitor the number of particles in a subvolume by a signal F which is proportional to N, (*b*) to measure the signals F_i from a sufficiently large number ($i = 1, \ldots, m$) of independent subvolumes, and (*c*) to monitor fluctuations of these signals in time, $F_i(t)$.

The spatial variations $\delta F_i = F_i - F$ are then related to the average number of particles N in volume V by

$$\overline{(\delta F_i/F)^2} = 1/N \tag{1}$$

and to the average density n and the molar weight M_p of the particle by

$$n = N/V = [\overline{(\delta F_i/F)^2}\, V]^{-1} \tag{2}$$

$$M_p = Ac/n = Ac\overline{(\delta F_i/F)^2}\, V, \tag{3}$$

where c is the weight concentration of the particle and A is Avogadro's number.

The change of fluctuation with time

$$\delta F_i(t) = F_i(t) - \langle F \rangle$$

at time t and

$$\delta F_i(t + \Delta t) = F_i(t + \Delta t) - \langle F \rangle$$

at time $(t + \Delta t)$, for any subvolume i, is described by the autocorrelation function

$$g_i(\Delta t) = \langle \delta F_i(t) \cdot \delta F_i(t + \Delta t) \rangle / \langle \delta F_i(t) \rangle^2. \tag{4}$$

This function decays to 0 when the delay time t becomes sufficiently long. The delay time $\Delta t_{1/2}$ at which half the number correlation is lost, $g_i(\Delta t_{1/2}) = 1/2\, g_i(0)$, defines the diffusion coefficient of the particle:

$$D = A_{cs}/\Delta t_{1/2} \tag{5}$$

where A_{cs} is an area which is related to the cross-section of the subvolume V. Thus, the signals $F_i(t)$, $i = 1, \ldots, m$ from m independent subvolumes V allow, in principle, the simultaneous and independent determination of

the number of independent particles in that volume N (and therefore the particle density n and the molar weight M_p) and of diffusion constant D.

Association and dissociation of particles lead, at constant mass density c, to changes in the average number of independent particles N (or n, or M_p). Therefore, observed changes of N are a direct measure for the average degree of occurring association or dissociation, η:

$$\eta = (c_1/c_2)\,[\langle(\delta F/F)^2\rangle]_1/[\langle(\delta F/F)^2\rangle]_2, \qquad (6)$$

where 1 and 2 refer either to different times ($c_1 = c_2$) or to different conditions. For, the case of a complete dimerization of monomers the value of η would be 2. For distributions of the aggregate size η measures average values (for evaluation of η for particular distributions see Petersen, 1986*a*). Changes of lateral diffusion constant D after association or dissociation may be determined as a function of η, $D(\eta)$. The above expressions for particles distributed in three dimensions apply as well to particles in two-dimensional systems, like membranes or surface monolayers. In the latter case, n and c are replaced by the surface concentrations of the number (n_s) and weight of particles (c_s), respectively, and the subvolume V is to be replaced by a "subarea" A_s.

Experimental Realization

The experimental approach for collecting and processing the required set of signals $F_i(t)$, $i = 1, \ldots, m$, is schematically shown in Fig. 1, and a diagram of the instrument used is given in Fig. 2. A rotating laser beam with gaussian intensity profile is focused on a thin cell of thickness h (or a surface adsorbed lipid/protein monolayer or membrane) containing fluorescent particles. During rotation (revolution time T_0 and length L), the collected fluorescence signal F fluctuates, $F(x)$, due to random variations of particle density along pathway x (Fig. 1 *a*). The spatial autocorrelation function

$$g(\Delta x) = [\overline{F(x)F(x + \Delta x)} - F^2]/F^2 \qquad (7)$$

of the fluorescence signal with mean amplitude F is schematically shown in Fig. 1 *b*. For a frozen sample (i.e., no diffusion), $g(\Delta x)$ would be strictly periodic in shape and amplitude with period L, since every pair of signals, distant by $\Delta x = k \cdot L$ or $\Delta t = k \cdot T_0$, $k = 0, 1, 2, \ldots$, would be identical, that is, fully correlated. Diffusion of particles will cause a loss of correlation with increasing delaytime $\Delta t = k \cdot T_0$. Consequently the correlation peaks drop in amplitude with increasing delay. Thus, the autocorrelation function for cyclic excitation of fluorescence contains both ensemble and time information: spatial variance of particle density is measured by the height of the zero-correlation peak, yielding N, n, and M_p, and fluctuations in time cause decreasing peak heights with increasing $\Delta x = k \cdot L$, $k = 1, 2, \ldots$, yielding diffusion constant D. For a formal justification of this data extraction, we have derived the following closed-form analytical expression for the autocorrelation function applying to cyclic excitation by a laser beam of gaussian profile. We start from the general expression

$$g'(\Delta t) = \left\{1/(c^2I^2)\int\int c[(\mathbf{r}';t)\, I(\mathbf{r}';t') \cdot c(\mathbf{r}'';t' + \Delta t)\, I(\mathbf{r}'';t' + \Delta t)\, d\mathbf{r}'\, d\mathbf{r}''\right\} - 1,$$

with the condition $I(\mathbf{r};\phi;t' + \Delta t) = I(\mathbf{r};\phi - 2\pi\Delta t/T;\, t')$ (ϕ: angle in radial coordinates). Since the beam radius w is necessarily much smaller than the radius of rotation, i.e., $w \ll r_0 = L/(2\pi)$, curvature effects may be neglected during integration using the coordinates

$$y = r - L/(2\pi), \qquad x = tL/T_0.$$

Similarly, detection of diffusion by partial loss of correlation after one turn necessitates that the passage time through each subvolume $\tau_0 = T_0 \cdot w/L$ must be set much smaller than the diffusion time out of each subvolume $\tau_D = w^2/(4D)$. At the same time tis allows to replace the variable Δt by the spatial position Δx. The resulting condition $T_0 \ll wL/(4D)$ considerably simplifies the integration yielding $g(\Delta x) = g(\Delta t \cdot L/T_0) = g'(\Delta t)$. Using a gaussian intensity profile $I(x, y)$ with the value of $I(z)_{x,y}$ constant, we find the following expression

$$g(\Delta x) = (1/N)[1 + 4DT_0k/w^2)^{-1} \cdot \exp[-(\Delta x - kL)^2/(w^2 + 4kDT_0)] \qquad (8)$$

with $N = \pi w^2 hn$ for particles in solution

or $N = \pi w^2 n_s$ for particles in membranes

h = cell thickness (optical path length)

$w = 1/e^2$ radius of the laser beam in sample

T_0, L = time and length of one rotation

k = integer (0, 1, 2, 3 . . .) to assign peaks.

The amplitudes of the correlation peaks are given by

$$g(kL) = (1/N)(1 + 4kDT_0/w^2)^{-1}. \qquad (9)$$

The average number of particles per subvolume (or subarea) is then given by

$$N = 1/g(0), \qquad (10)$$

and the lateral diffusion constant D can be determined from any pair of peaks, such as, $g(0)$ and any $g(kL)$, $k = 1, 2, 3 \ldots$ according to

$$D = [w^2/(4T_0k)][g(0)/g(kL) - 1] \qquad k = 1, 2, \ldots \qquad (11)$$

For completeness, relations 2 and 3 for particle density and molar weight now read

$$n = [g(0)\pi w^2 h]^{-1} \qquad (12)$$

$$M_p = Acg(0)\pi w^2 h. \qquad (13)$$

For application to monolayers or membranes h is omitted and n and c are

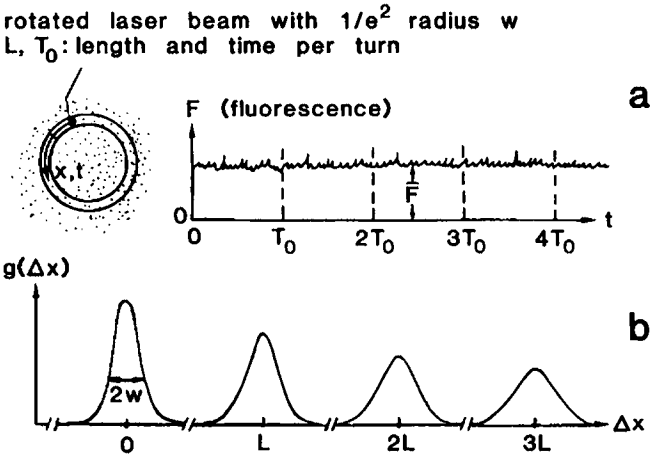

FIGURE 1 Schematic illustration of circular signal collection, fluctuating signal F, and of the correlation function $g(\Delta x)$ of signal F. The average density of fluorescent particles is obtained from the width w and the height of the zero correlation peak $g(0)$, while the lateral diffusion constant of the particle is evaluated from the decay of the peak heights with increasing Δx.

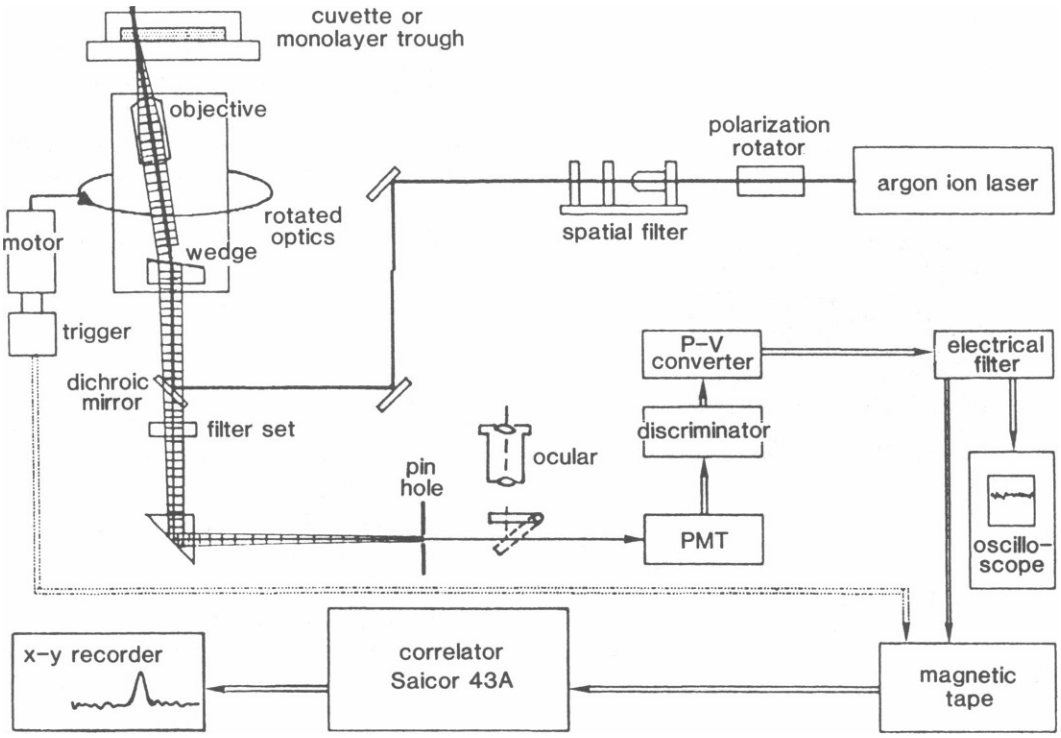

FIGURE 2 Schematic of the experimental apparatus. The optical design of the FPC apparatus is based on an inverted fluorescence microscope. The light source is a stabilized argon laser (model 166-08, 5 W; Spectra-Physics Inc., Mountain View, CA) at 476 nm. Rotation of the laser-polarization into the horizontal plane increases the reflection properties of the dichroic mirror (see below). The spatial filter (No. 22-6035; Ealing Corp., S Natick, MA) is used for beam expansion and shaping (gaussian beam profile). The filter set below the dichroic mirror (No. 30446, edge 505 nm; Balzers, Hudson, NH) consists of a band pass filter (No. 100554.03; Schott Glass Technologies Inc., Duryea, PA) and two high pass filters (Schott, KV 500) to eliminate scattered light and the Raman line of water. The objective, specially constructed in the laboratory (Meyer, 1986), is composed of three quartz lenses. It is optimized for high numerical aperture (0.45) at a working distance of 14 mm, an objective to image distance of 700 mm, and a magnification of 25.4. Fluorescence detection is performed by a Hamamatsu Corp. (Middlesex, NJ) R-464 single photon photomultiplier (efficiency at 520 nm ~5%). Unwanted fluorescence (emitted mainly from the dichroic mirror) is rejected by an adjustable diaphragm in the image plane. The spot size in the object plane is adjustable by moving the second lens of the spatial filter (smallest $1/e^2$ spot radius 3.1 μm). Fine adjustments of the two mirrors and of the dichroic mirror allow for imaging the illuminated sample volume on the diaphragm. The wedge (quartz) deflects the incident beam and the collected fluorescence by 1 degree. The distance between the wedge and the object plane is 118 mm. Wedge and objective are mounted on a cylindrical unit, which fits into a playless rotation device. The pedestal of this device is vertically adjustable to image the object in the diaphragm plane. Rotation of optics is performed by a tooth wheeled device driven at 4 times reduction by a stabilized motor. For signal analysis a correlator is used (Saicor 43A; Honeywell Information Systems Inc., Waltham, MA). The discriminated single photon pulses are converted to an anlog signal (No. 9349 with low pass filter, EG&G Ortec, Oak Ridge, TN) and stored on magnetic tape (Racal 4D; Racal Recording Inc., Irvine, CA). The angular pulses during rotation (ZR-500; Zivy and Co., Muenchenstein, Switzerland) are stored on tape, in parallel with the fluorescence signal. They are used as trigger pulses for the delayed, positional correlation analysis. The storage space of the autocorrelator alows to store five correlation peaks (2,000 pulses per rotation). A Teflon trough for measurements on monolayers can be mounted on top of the housing. A plane concave quartz lense is imbedded in the bottom of the trough, sealed by a Teflon earring. The trough is supplied with two surface barriers and a Wilhelmy plate balance (Transducer SS101; Collins Corp., Long Beach, CA) to monitor surface pressure. A peristaltic pump to fill the trough and vacuum suction by a thin glass pipette are used to define a precise surface level and to clean the surface before monolayer formation. For measurements in solution, the upper half of a 10-μm cuvette (Hellma Cells, Inc., Jamaica, NY) is pressed on the plano-concave lens by a heavy, hollow cylinder. A scrupulous cleaning procedure using chromosulfuric acid is applied to the cuvette, the lense, and the Teflon trough before experiments.

replaced by the surface densities n_s and c_s, respectively. Finally, relation 6 for the degree of association or dissociation reads now

$$\eta = (c_1/c_2)g(0)_1/g(0)_2. \quad (14)$$

Except for concentration c (or c_s) and cell thickness h, all quantities needed to determine N, D, n, M_p, and η are taken directly from the measured correlation function $g(\Delta x)$. There is no need to independently determine the area πw^2 or volume $\pi w^2 h$, since w is obtained from the $1/e$ width of the autocorrelation peak (see Eq. 8 and Fig. 3). Background fluorescence (B) is easily introduced in all formulas by using $g(0)/(1 + B/F)^2$ instead of $g(0)$, since

$$g(0) = \delta F^2/(F + B)^2 = g(0)_{B-0}/(1 + B/F)^2, \quad (15)$$

where B/F can be determined from experiments without and with fluorescence label at identical conditions otherwise.

RESULTS AND DISCUSSION

Particles in Solution

Eqs. 11 to 13 for data evaluation contain w as an effective diffusion length and πw^2 as effective area for determining particle density or molecular weight. According to the theory (Eq. 8) w is directly obtained from the $1/e$ width of the zero correlation peak $g(\Delta x)_{k-0}$ with gaussian shape,

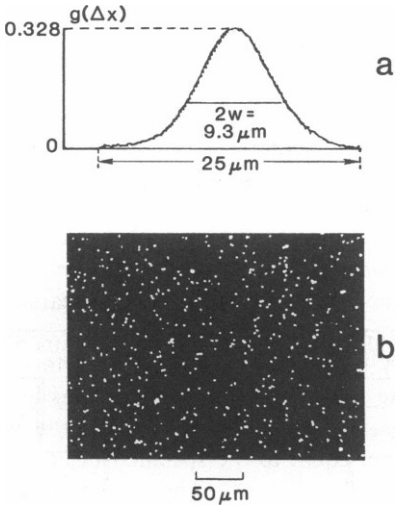

FIGURE 3 Comparison of the density of latex beads (1.13-μm diam) obtained from FPC (*a*) and from fluorescence microscope photographs (*b*). (*a*) T_0 = 31.1 s, number of rotations K = 20, B/F = 0.02, bead concentration c = 2.84 mg/ml. (*b*) Bead concentration 5.5 times diluted: c = 0.516 mg/ml, 1,070 beads were counted over 100 cm^2 of a photograph at a magnification of 276.3.

provided the intensity distribution of the laser beam is gaussian. This built-in calibration of effective area or length has been put to experimental test in the following way: FITC-labeled latex beads of 1.13-μm diam were counted using FPC and from photographs using a fluorescence microscope, see Fig. 3, *a* and *b*. In both cases the same cell was used. The sample used in the photograph was 5.5 times diluted for more reliable counting of beads. The density on the photograph was 8.2×10^5 beads/cm^2 with 1,070 beads counted. From the amplitude $g(0) = 1/N = 0.328$ and $1/e$ peak-width corresponding to $w = 4.65$ μm, a density of 4.49×10^6 particles/cm^2 ($\approx 5.5 \times 8.2 \cdot 10^5$/$cm^2$) was calculated. A match with a 10% accuracy was found for spot sizes between w = 3.5 and 50 μm. At w = 3.5 μm where the laser beam is focused to the center of the cell, so that w is expected to change within the cell of thickness h, one would estimate a 6% change from the relation $(\Delta I/I)_{max} = 1 - [1 + h\lambda/(2\pi w^2)]^{-1}$ (see Chu, 1974). Although the distribution of w values along the beam axis about the focus is not gaussian, the resulting correlation peak was, within experimental errors, always gaussian. We conclude from this that w provides as accurate a measure for effective length and area as independent calibration experiments do. The error in reading w is set by the noise in the correlation peak, typically ~1% (Fig. 3 *a*).

Molar Weights of Particles

From the peak height $g(0)$ and width w of Fig. 3 *a*, at the concentration c = 2.84 (±0.03) mg/ml and specified cell thickness h = 10 μm the molar weight of the 1.13-μm latex beads is calculated from Eq. 13 to be $3.80\ (\pm 0.4) \times 10^{11}$ D (the error is due to systematic uncertainties as addressed below). For 0.1-μm latex beads (see Fig. 4 *a*), a molar weight of $3.67\ (\pm 0.4) \times 10^8$ D was determined. There are no specified molar weights for these beads, but they can be estimated from density and diameter, assuming spherical shape to be 4.5×10^{11} and 3.2×10^8 D, respectively. These values differ by 15% from the FPC data, which is certainly within the error limits of this estimate. In Fig. 4 *a* two $g(0)$ peaks are shown. They have been obtained from the identical data set (stored on tape). In the left peak time correlation is used for a more precise estimate of the amplitude $g(\Delta x)_{k=0}$, since in time correlation the number of data points per peak can be set to up to 400 with the correlator used, whereas the number of data points in position triggered correlation is limited by the 2,000 trigger positions per rotation. Fig. 4 *b* shows data points obtained with BSA-FITC at 26 (±1.3) ng/ml. The number of labeled BSA molecules per spot $N = g(0)^{-1}$ is 3,850 (±120), w = 21.9 (±0.6) μm. The resulting molar weight is 61,000 with an error of 10%, which compares to the known value 64,000 D. (An independent preparation yielded a value of 64,000 (±6,000) D.)

In the same way molecular weights of aldolase, thyroglobulin, and of the FITC-label itself has been measured. These results are tabulated in Fig. 5 to illustrate the enormous range of molar weights measurable by this method. From the signal-to-noise analysis outlined below and from the design of the present apparatus, particle weight determination by FPC is characterized by: (*a*) no limit to particle weight; (*b*) one FITC label per particle is sufficient; (*c*) accuracy is routinely 10% and 5% at optimized conditions; (*d*) particle concentration should be between 10^{-10} and 10^{-7} M; (*e*) sample volume per measurement 100 μl; (*f*) typical measurement time 1–3 min. One of the largest uncertainties is the thickness of the purchased cell used for all experiments. It is specified as 10 (±1) μm. The presented data on molecules of known molecular weight (BSA, aldolase, thyroglobulin, and

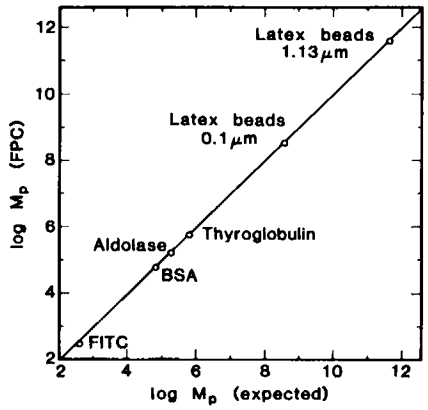

FIGURE 4 Correlation functions $g(\Delta x)$ measured for latex beads (*a*) and for FITC-labeled BSA (*b*). (*a*) Bead diameter 0.1 μm, w = 25.65 μm, T_0 = 21.9 s, K = 20, B/F = 0.01, bead concentration c = 23.7 μg/ml. (*b*) BSA concentration c = 26 ng/ml (p = 4), w = 21.9 μm, T_0 = 3.13 s, K = 65.5, B/F = 0.51, incident laser power 20 mW, 500 μg/ml unlabeled BSA.

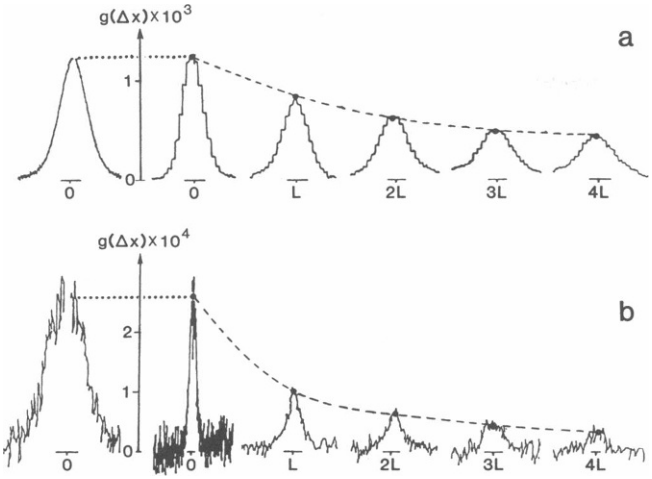

FIGURE 5 Molar weights measured by FPC plotted against expected values. Measured and expected values are: FITC: 302 (±30)–389; BSA: 62,600 (±6,000)(average of two preparations)–64,000; Aldolase: 162,000 (±16,000)–158,000; Thyroglobulin 610,000 (±60,000)–669,000. Conditions for these FITC-MW determinations see text and Methods section. Latex beads, 0.1 μm: 3.67 (±0.4) × 10^8–3.2 × 10^8; Latex beads 1.13 μm: 3.8 (±0.4) × 10^{11}–4.5 × 10^{11}. Expected weights for latex beads are derived from size and specific weight.

FITC) suggest a cell thickness of 10.5 μm since this value gives best fit of the FPC data to the known values.

Simultaneous Determination of Particle Weight and Lateral Diffusion

Fig. 4 shows two examples for data from which particle weight and lateral diffusion can be evaluated. Values of D are obtained according to Eq. 11 from w and the heights of the correlation peaks $g(kL)$. The best fit is indicated by dots and dashed lines. For the 0.1-μm latex beads in Fig. 4 *a*, a value of 4.2(±0.4) × 10^{-8} cm^2/s is found, which compares well with the expected value (see Table I). These data were obtained with positional triggering. When using the delay time of the autocorrelator instead of the positional trigger, the delayed peaks were reduced or invisible. This is due to the earlier mentioned technical difficulty in turning the optics at sufficiently constant speed, which results in a broadening and amplitude reduction of the delayed correlation peaks. The value D_{FCS} was measured by holding the optics stationary and observing density fluctuations in time at one spot (w = 18.4 μm). For this stationary measurements of the FCS type (pure time correlation, no position correlation), a similar accuracy in the determination of D could be reached after a 3 h measurement, whereas the determination of D_{FPC} lasted 3 min. This time difference is due to collection of fluctuating signals from not one but several hundred independent volumes (L/w, here 500). In stationary FCS, the time spent dwelling on a spot between $t = 0$ and τ_D is partially wasted, because little new information (apart from overcoming photon statistics noise) is obtained in time intervals much smaller than the sample correlation time. This spare time can be effectively utilized by scanning into and observing new volumes, each of which are visited only occasionally.

TABLE I

Particle	$D_{expected}$	D_{FPC}	D_{FCS}
	$\mu m^2/s$	$\mu m^2/s$	$\mu m^2/s$
Latex beads, 1.13 μm	0.38	0.39 ± 0.04	0.39 ± 0.04
Latex beads, 0.1 μm	4.3	4.2 ± 0.4	4.7 ± 0.5
BSA	61	57 ± 6	—

The value of $D_{expected}$ for latex beads has been calculated from the relation $D = kT/(6\pi\eta r)$ where the hydrodynamic radius r is set equal to the specified bead radius and η = 0.01 poise at T = 293.2°C. The measured values for both bead sizes match this expectation. For BSA, Fig. 4 *b*, the measured value is also in reasonable agreement with data from the literature (Wagner and Scheraga, 1956). The experimental signal-to-noise ratio in Fig. 4 *b* is taken from the root-mean-square noise between peaks (rms), $S/N = g(0)/\text{rms} = 14$ which is compared below with theoretical predictions. It is apparent from Fig. 4 that the $1/e$ width of the k-peak ($w_{k,exp}$) increases with increasing k. This is predicted by the theory. From Eq. 8 this diffusion broadening ($w_{k,th}$) should follow the relation

$$w_{k,th} = w_0(1 + 4DT_0k/w_0^2)^{1/2}. \quad (16)$$

Using the data in Fig. 4 *a* this relation is accurately confirmed since

$$w_{k,exp}/w_{k,th} = 1.00 \pm 3.5\% \text{ (standard deviation)}.$$

For the present FPC apparatus, measurable diffusion constants fall into the range of 10^{-7} to 10^{-10} cm^2/s, with an error of 5–10% (increasing with increasing D). These limits are determined by the limited range of rotation speeds obtainable by the present apparatus and the limited number of positional trigger signals per rotation. Because of these limitations, w cannot be much smaller than 10 μm for measurements of diffusion constants. With FPC, D is directly determined from $g(\Delta x)$, without independent determination of w as required in FCS experiments. The optimal choices for parameters to simultaneously measure M_p and D are discussed below.

Aggregation of Particles: Calcium Dependence of Lipid Vesicle Fusion

Fluorescence particle counting is, strictly speaking, a method to determine not the molecular weights but rather the average molar weight of independently distributed particles in solution or in membranes. In the examples so far chosen, agreement between the M_p values and the known molar weights show that the molecules were singly distributed at random (most particles consist of one molecule) and that no aggregation occurred during the time of

the experiment. If aggregation had taken place, it should have been detectable by an increase of $g(0)$, proportional to the average aggregation number described by η (see Eq. 14) and also by a change of D from amplitude changes of the following peaks $g(kL)$. This application to monitor aggregation may be illustrated using data obtained with lipid vesicles (Fig. 6). Lipid vesicles were made by sonication from POPC/DOPS (1:1, wt/wt) with 1.2 wt% PC-NBD as the fluorescent probe. A 4× dilution series from 700 to 0.17 μg/ml was performed to study concentration- and Ca^{2+}-dependent vesicle aggregation. The samples were incubated for 90 min at 37°C and the aggregation number was then measured in the FPC (Fig. 6). The data shown refer to the $g(0)$ peaks found for these conditions; data on lateral diffusion $g(kL)$ are not included. Particle densities n were measured according to Eq. 12. The average number of lipids per particle is then $\eta_{lip} = n_e/n$ (special case of Eq. 14), where n_e is the known number density of total lipid in solution. In the absence of Ca^{2+} or without any incubation, the number of lipids per particle is $\sim 10^4$. This value corresponds to small unilamellar vesicles of ~350-Å outer diam (at 70 Å^2/lipid) which is expected to result from heavy sonication of the lipid mixture used. Incubations in the absence of Ca^{2+} show almost no vesicle aggregation; the vesicle-aggregation number η_{ves} remains close to 1 even at high vesicle concentrations. In the presence of Ca^{2+} vesicles tend to aggregate in a concentration-dependent manner. Below 20 μg/ml lipid concentration an average of 18 vesicles aggregated or fused with little dependence on concentration. Above 20 μg/ml an additional concentration-dependent increase in particle weight occurs. Up to 120 vesicles aggregated (fused) under these incubation conditions. From the data in Fig. 6 it cannot be determined to what extent the Ca^{2+} effect on aggregation (18-fold increase) and the concentration effect

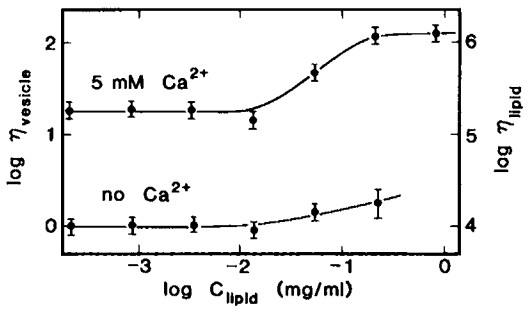

FIGURE 6 Average particle size in a lipid vesicle suspension as a function of lipid concentration, in the absence and presence of Ca^{2+}. Vesicles were prepared by sonication of POPC and DOPS (1:1, wt/wt with 1.2 wt% PC [NBD-labeled]) in a buffer containing 100 mM NaCl (for details see Materials and Samples). Samples were incubated for 90 min at 37°C with and without Ca^{2+}. The average number of lipids per particle (right scale η_{lipid}) was determined in the FPC for the concentrations of 4× dilution series. Before incubation 10^4 lipids/vesicle were measured (left scale $\eta_{vesicle}$). FPC parameters were: B/F depending on lipid concentration, w = 12.1 μm, T_0 = 12 s, K = 15.9. 500 μg/ml unlabeled vesicles (no PC-NBD) were added to prevent surface artifacts.

(additional sevenfold increase) relate to vesicle aggregation or to vesicle fusion. Association and fusion may be differentiated by assaying the most rigorous critera for vesicle fusion (coalescence of the internal compartment of vesicles, Duzgunes et al., 1981, and the concomitant mixing of membrane lipids) by fluorescence quenching in conjunction with the same type of FPC measurements described above. FPC can be used as a powerful method to further investigate the question of Ca^{2+}-induced membrane–membrane association and fusion (for phosphatidylserine vesicles see for example Kachar et al., 1986; Day et al., 1977; Wilschut et al., 1981). For changes in particle weight with changing conditions as exemplified above, the same characteristics and limits apply as mentioned at the end of the section "Molar Weight of Particles" above. Changes of particle weight in time at constant conditions may also be assayed, provided they occur sufficiently slow (i.e., in minutes).

FPC on Two-dimensional Systems: Aggregation of Matrix Protein from *E. Coli*

Application of FPC to two-dimensional systems is illustrated by measurements of the aggregation of a membrane protein, matrix protein from *E. Coli* outer membranes. Matrix protein was chosen because it is well known to form large aggregates and even two-dimensional crystals (Garavito and Rosenbusch, 1980; Engel et al., 1985) in lipid membranes and to form arrays of ion channels when co-associated with lipopolysaccharide (LPS) both in reconstitution and in native membranes (Schindler and Rosenbusch, 1978, 1981).

The experimental procedure for following matrix protein aggregation in time (Fig. 7 *a*) was essentially as follows (for details see Methods section): Instead of a sample cell a monolayer trough was used. Monolayers were generated from vesicles containing lipid and matrix protein trimers (MX_3, FITC-labeled) in such a way that the MX_3 molecules were expected to be randomly distributed within the monolayer. Starting from this initial condition ($t = 0$) aggregation of MX_3 was followed by consecutive measurements of $g(0)$, where each measurement took 32 s (horizontal error bars in Fig. 7 *a*). The average number of MX_3 per aggregate, η_{MX3}, is obtained from $\eta_{MX3}(t) = mg(0)_t$, where m is the average number of MX_3 per spot, calculated from the lipid to protein molar ratio (r) and the area per lipid (a) according to $m = \pi w^2/(ra)$. The data in Fig. 7 *a* were obtained at m = 7 MX_3/spot.

Aggregation was followed for 2 h, during which η_{MX3} increased to 700. The onset of aggregation was too fast to be measured completely. During the first measuring period at ~1 min, η_{MX3} was already 30 (an earlier start of the measurement is not possible due to the time needed to spread the monolayer).

Fig. 7 *b* shows changes of MX_3 aggregate size as a function of monolayer pressure π and lipid composition. After pressure changes 5 min were allowed for equilibra-

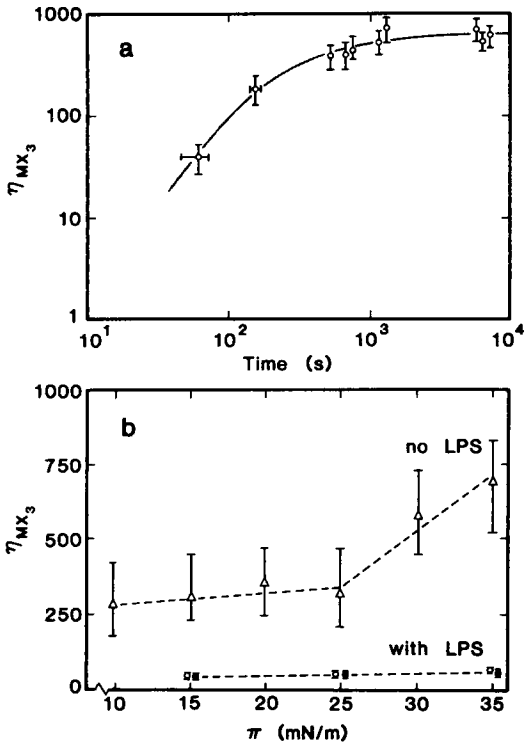

FIGURE 7 Formation of large matrix–protein aggregates in lipid monolayers, followed as a function of time (*a*) and as a function of surface pressure π at different lipid compositions of the monolayer (*b*). (*a*) Molar ratio matrix protein trimer (MX_3, FITC-labeled): soybean lipid was $1:10^7$. The MX_3 molecules were randomly distributed at time 0 within the monolayer plane, at monolayer pressure π = 25 mN/m (see text). Horizontal error bars indicate the time intervals of signal collection (32 s each). The signals were stored on tape and later analyzed to yield $g(\Delta x)$ functions from which average numbers of MX_3 molecules per particle (η_{MX3}) were calculated with the accuracy indicated by the verticle error bars. FPC parameters were: B/F = 20 (due to fluorescence of soybean lipid), w = 4.1 μm, T_0 = 14 s, K = 2.2, p = 2.6. (*b*) *Upper curve:* Molar ratio MX_3-FITC/DMPC; $1:1.5 \times 10^6$. The increase of the average MX_3 aggregation number η_{MX3} with increasing surface pressure π above 25 mN/m was reversible (see text). *Solid circles,* mean values; *error bars,* the total range of three independent determinations of η_{MX3} using the monolayer. The lower data were obtained in the presence of lipopolysaccharides (LPS) at a molar ratios MX_3/LPS/DMPC of $1:10:10^5$ (*open circles*) and $1:10^3:10^5$ (*solid circles*). FPC parameters were: B/F = 1.3 (*upper*), 0.2 (*lower curve*), w = 4.1 μm, T_0 = 14 s, K = 8.8.

tion. The lipid DMPC is used at molar ratios DMPC/MX_3 of 1.5×10^6 (*upper data*) and 10^5 (*lower data*). The upper curve (no additional lipopolysaccharide) shows that the average aggregate size is dependent on surface pressure π. The experiment was started at π = 35 mN/m, where η_{MX3} was ~700. This value dropped to ~300 when pressure was relaxed to 25 mN/m and stayed at this value for lower pressures down to 10 mN/m. The process was reversible, since η_{MX3} increased again when the pressure was raised to above 25 mN/m. The error bars cover the range of three independently determinated values (taken at different time but with the same monolayer preparation) and the filled circles represent the mean values.

Vesicle preparation in the presence of LPS (*lower curve*) had two effects: it abolished the small pressure effect, and it reduced the apparent aggregate size to ~50. This reduction was in spite of the fact that the MX_3 density was higher by a factor of 15. This effect of LPS is apparently already saturated at a molar ratio LPS/MX_3 of 10 (*open circles*). Increasing the LPS content by a factor 100 had no additional effect (*solid circles*). This finding shows that LPS, which is known to be co-associated with MX_3 and to be essential for ion channel function (Schindler and Rosenbusch, 1981), indeed reassociates with MX_3 to form a different type of complex than formed by MX_3 alone, with smaller and pressure insensitive size.

SIGNAL-TO-NOISE AND PARAMETER OPTIMIZATION

In FPC experiments for specific applications, it is not obvious at which values of the free parameters (laser intensity I, spot radius w, time per turn T_0, number of turns K) and also of particle concentration c and of label per particle p (with certain labeling variance) application is feasable and optimized with respect to the signal-to-noise ratio. Relations derived from signal-to-noise considerations should considerably facilitate the appropriate choice of parameters and variables. Such relations should allow to determine whether a setup of this kind is sensitive enough to count particles. A detailed analysis (Meyer, 1986) reveals that the following parameters are the important ones to be optimized for applications:

$$\gamma/\alpha, \qquad (1 + B/F)^{-1} \qquad \text{and} \qquad N_0^{1/2}.$$

γ is the cross-section of an independent labeled particle (molecule) for detection of an emitted fluorescence photon (cross-section for absorbance × quantum yield × probability of detection); α is the cross-section for bleaching (irreversible photo-destruction) of the dye; B/F is the ratio of the background (no label on sample) to the average fluorescence signal; N_0 is the number of independent volumes (areas) to be sampled.

To deduce the quantitative relations, we start with a simplified model (for another approach to determine S/N ratios see also Koppel, 1974); (*a*) no diffusion of labeled molecules, (*b*) a homogeneously illuminated area (volume), (*c*) circular collection of photons from independent, succesively illuminated areas (volumes), (*d*) one data point is collected from each spot, (*e*) there are M spots per turn and K turns yielding KM digitally sampled values. The signal-to-noise ratio (S/N) will be calculated for the number noise in the first correlation peak (1 turn delay) where photon shot noise does not contribute to the peak height. The correlation signal is then given by

$$S = 1/(f^2N^2)\ 1/(KM) \sum_{m=1}^{M} \sum_{k=1}^{K} (n_{m,k} \cdot n_{m,k+1} - n_{m,k} \cdot n_{m+1,k+1}); \qquad \langle S \rangle = 1/N, \quad (17)$$

where $n_{m,k}$ is the number of collected photons in spot m at

rotation k, and f is the number of detected photons per particle per second, i.e.,

$$\langle n_{m,k} \rangle = \langle fN_m \rangle = f \cdot N.$$

The second term in Eq. 17 is a product of noncorrelated data. S/N can then be obtained from the average signal, $1/N$, divided by its variance

$$(S/N) = (1/N)\,(\langle S^2 \rangle - \langle S \rangle^2)^{-1/2}. \qquad (18)$$

The number of collected photons from a fluorescent source in any practical time interval is Poisson distributed (Koppel, 1974). Insertion of Eq. 17 into Eq. 18 leads to four products to be averaged separately. For example, one product is $\langle n_{m,k} \cdot n_{m,k+1} \cdot n_{r,s} \cdot n_{r,s+1} \rangle$. This again splits into a sum of several averages for suitable relations between indices, which can be directly evaluated. For example, for a number MK of all possible choices (M^2K^2), the relation between the indices is $r = m$, $s = k + 1$, leading to

$$\langle nm,kn^2_{m,k+1}n_{m,k+2} \rangle m,k = \langle f^4N^4_m + f^3N^3_m \rangle m$$
$$= f^4(N^4 + 6N^3 + 7N^2 + N) + f^3(N^3 + 3N^2 + N).$$

Calculating all terms of Eq. 18 one obtains an S/N ratio of

$$(S/N) = \left[\frac{3 + 1/N}{M} + \frac{6 + 4/N}{MKf} + \frac{2 + 1/N}{MKf^2}\right]^{-1/2}. \qquad (19)$$

With $N \gg 1$ for most applications, this relation simplifies to

$$(S/N) = [(2 + 6f)/MKf^2 + 3/M]^{-1/2}. \qquad (20)$$

The first term depends on the total number of collected photons and the second term on the number of independent subvolumes. These two terms can be separated into two noise contributions corresponding to photon statistics noise $(S/N)_1$ and noise due to an insufficient number of independent subvolumes from which data were sampled $(S/N)_2$:

$$(S/N)_1 = f\,[MK/(2 + 6f)]^{1/2} \qquad (S/N)_2 = (M/3)^{1/2}. \qquad (21)$$

These general relations are changed into more practical ones by introducing: (a) $M = L/w$; (b) $f = \gamma I_0 \tau_0/(\pi w^2)$, where I_0 is the incident light intensity (number of photons per second), γ is the cross-section for the detection of an emitted fluorescence photon and $\tau_0 = T_0/M$; (c) the effect of diffusion is to increase the number of independent volumes M by a factor of approximately $(1 + 4DKT_0/w^2)$; (d) background fluorescence is taken into account by multiplying $(S/N)_1$ by $(1 + B/F)^{-1}$ (see Eq. 15); $(S/N)_2$ is not dependent on background fluorescence B. Eq. 21 now reads

$$(S/N)_1 = 0.23\gamma I_0 T_0 K^{1/2} w^{-3/2} L^{-1/2}\,(1 + B/F)^{-1}$$
$$(S/N)_2 = (L/3w)^{1/2}[1 + 4DKT_0/w^2]^{1/2}. \qquad (22)$$

The next step is to introduce fluorescence bleaching which gives a limit to I_0. Bleaching is assumed to reduce γ:$\gamma(t) = \gamma_0 \exp\,[-\alpha I(x, y)t]$, where α is the bleaching cross-section, $I(x, y)$ is the gaussian distributed intensity. In first order approximation bleaching reduces fluorescence F by $F(t) = F_0\,(1 - \alpha I_0 t/\pi w L)$, where w may be replaced by $(2DKT_0)^{1/2}$ if the sample diffuses.

Although bleaching reduces $F(t)$, it has only a secondary effect on $g(\Delta x)$, since it is based on fractional fluctuations $\delta F/F$. It can be shown (Meyer, 1986), that a 25% bleaching of fluorescence reduces $g(0)$ by 4%. Therefore, maximal reduction of $g(0)$ by 4% limits the intensity to

$$I_0 < 0.6(L/\alpha)(D/KT_0)^{1/2}$$
$$= (0.3/\alpha)(Lw/T_0)K^{-1/2} = I_{0,\mathrm{lim}}, \qquad (23)$$

where D is set equal to $w^2/4T_0$ for which $g(0)/g(L) = 2$, the optimal condition to evaluate D. Insertion of this intensity limit in Eq. 22 yields the final S/N expressions:

$$(S/N)_1 = 0.07 \cdot (1 + B/F)^{-1} \cdot (L/w)^{1/2} \cdot \gamma/\alpha$$
$$(S/N)_2 = [L(1 + K)/(3w)]^{1/2} \quad \text{at} \quad T_0 = w^2/(4D). \qquad (24)$$

These relations are fundamental to understand the limitations on a wide range of fluorescence application. In this study, they were used to optimize the design of the FPC apparatus and to determine the feasibility of a specific FPC experiment. For FITC, mostly used here, γ and α were measured to be $\gamma = \bar{p} \cdot 3.0 \times 10^{-21}$ cm^2 (factor $\bar{p}$ denotes the average number of FITC labels per particle) and $\alpha = 6.0 \times 10^{-22}$ cm^2 in the presence of radical scavenger (1 mg/ml p-phenylediamine, used in all examples described here). The length per rotation L is fixed in our apparatus to be 1.29 cm. Therefore, for the data described, the (S/N) relations become

$$(S/N)_1 = 40(\bar{p}/w[\mu\mathrm{m}]^{1/2})(1 + B/F)^{-1},$$
$$(S/N)_2 = 38[(1 + K)/w[\mu\mathrm{m}])]^{1/2}$$
$$\text{at} \quad T_0 = w^2/(4D). \qquad (25)$$

As an example, for the BSA data in Fig. 4 b ($w = 21.9$ μm, $K = 65.5$, $\bar{p} = 4$, $B/F = 0.51$) the expected signal-to-noise value is $(S/N) = [(S/N)_1^{-2} + (S/N)_2^{-2}]^{-1/2} = 21$. The experimental value was equal to 14.

It may be surprising that the number of molecules in the illuminated volume (N) does not enter the above S/N expressions (but see text to Eq. 20). N is limited to high values by systematic fluctuations of light source and detection system. These fluctuations have to be at least 4 times smaller than the observed number fluctuations. For our setup, this limit is $N < 5 \times 10^4$. The lower limit to N is set by the collection of background photons, primarily a question of unspecific background of the sample or secondary fluorescence of the optical filters used. This minimal background signal from the optical filters corresponded to the signal of a sample with a label density of 1 FITC

molecule per μ^2. The fluorescence of the sample should be at least a few times this value. This sets a lower limit to N of approximately: $N > 10 \cdot w \cdot [\mu m^2]/\bar{p}$. For example the BSA data in Fig. 4 *b* were obtained at $w = 21.9$ μm and $\bar{p} = 4$, giving a range of $10^3 < N < 5 \times 10^4$. The value used was 4×10^3.

So far we have not included the effect of variance in fluorescence labeling $\langle (p_i - \bar{p})^2 \rangle i$. It leads to an unwanted number noise and therefore to an underestimation of N but has practically no effect on S/N. The product of the optical extinction coefficient ϵ and the fluorescence quantum yield, ϵQ, can have a broad distribution in a labeled sample. It has been shown (Elson and Magde, 1974), that the peak height of the autocorrelation function is increased because of such a distribution by a factor of $\langle \epsilon Q)^2 \rangle / \langle \epsilon Q \rangle^2$. For a particle with p_0 equivalent binding sites and $\bar{p}$ labels bound on average (without self-quenching), the peak height is

$$g(0) = g(0)_{p-p_0} (1 + 1/\bar{p} - 1/p_0) \qquad (26)$$

derived from the binominal standard deviation. To minimize errors from this source, $\bar{p}$ must be sufficiently large ($\bar{p} > 10$), or, at $\bar{p} < 10$, binding should be at or close to saturation ($\bar{p} \sim p_0$), or, at $\bar{p} \ll 1$, the fraction of labeled particles (1 dye) may be determined measuring dye absorbance. With an average of four dyes bound (example BSA), the measured molecular weight could be up to 25% higher than the real value. At $\bar{p} = 4$, the binding of FITC to BSA was however, found to be close to saturation (without denaturing the protein). This is a posteriori confirmed by the comparison of measured and expected molecular weights.

The results presented here demonstrate some applications of the FPC method, along with its characterization in terms of the limitations on signal-to-noise imposed by background light, collection efficiency, bleaching, and the number of independent volumes. These results establish the inherent potential of this technique and lay the groundwork for its further development. The FPC approach complements previous methods in correlation and fluctuation spectroscopy and extends their range of applications in biology. It should be particularly useful in analyzing the aggregation of macromolecules, vesicles, and other particles in reconstituted systems. Measurements of the size and dynamics of multimeric complexes can contribute to the understanding of important biological processes such as receptor aggregation and vesicle fusion.

This work was supported by the Swiss National Science Foundation, grant 3303.82.

Received for publication 23 February 1988 and in final form 21 June 1988.

REFERENCES

Axelrod, D., N. L. Thompson, and T. P. Burghardt. 1983. Total internal inflection microscopy. *J. Microsc.* 129:19–28.

Cherry, R. 1979. Rotational and lateral diffusion of membrane proteins. *Biochim. Biophys. Acta.* 559:289–327.

Chu, B. 1974. Laser Light Scattering. Academic Press, Inc., New York. 155.

Day, E. P., J. T. Ho, R. K. Kunze, Jr., and S. T. Sun. 1977. Dynamic light scattering study of calcium-induced fusion in phospholipid vesicles. *Biochim. Biophys. Acta.* 479:503–508.

Duzgunes, N., S. Nir, J. Wilschut, J. Bentz, C. Newton, A. Portis, and D. Papahadjopoulos. 1981. Calcium and magnesium induced fusion of mixed phosphatidylserine/phosphatidylcholine vesicles: effect of ion binding. *J. Membr. Biol.* 59:115–125.

Elson, E. L., and D. Magde. 1974. Fluorescence correlation spectroscopy, I. Conceptual basis and theory. *Biopolymers.* 13:1–27.

Elson, E. L., and W. W. Webb. 1975. Concentration correlation spectroscopy: a new biophysical probe based on occupation number fluctuation. *Annu. Rev. Biophys. Bioeng. 4:311–334.*

Engle, A., A. Massalski, H. Schindler, D. L. Dorset, and J. P. Rosenbusch. 1985. Porin channel triplets merge into single outlets in Escherichia Coli outer membranes. *Nature (Lond.).* 317:643–645.

Garavito, R. M., and J. P. Rosenbusch. 1980. Three dimensional crystals of an integral membrane protein: an initial x-ray analysis. *J. Cell Biol.* 86:327–329.

Gross, D., and W. W. Webb. 1986. Molecular counting of low-density lipoprotein particles as individuals and small clusters on cell surfaces. *Biophys. J.* 49:901–911.

Handbook of Biochemistry and Molecular Biology, Proteins. Vol. II. 1976. G. D. Fasman, editor. CRC Press, Cleveland, OH.

Icenogle, R. D., and E. L. Elson. 1983. Fluorescence correlation spectroscopy and photobleaching recovery of multiple binding reactions. I. Theory and FCS measurements. *Biopolymers.* 22:1919–1948.

Kachar, B., N. Fuller, and R. P. Rand. 1986. Morphological responses to calcium-induced interaction of phosphatidylserine containing vesicles. *Biophys. J.* 50:779–788.

Koppel, D. E. 1974. Statistical accuracy in fluorescence correlation spectroscopy. *Phys. Rev. A.* 10:1938–1945.

Koppel, D. E., D. Axelrod, J. Schlessinger, E. L. Elson, and W. W. Webb. 1976. Dynamics of fluorescence marker concentration as a probe of mobility. *Biophys. J.* 16:1315–1329.

Magde, D., E. L. Elson, and W. W. Webb. 1974. Fluorescence correlation spectroscopy, II. An experimental realization. *Biopolymers.* 13:29–61.

Meyer T. 1986. Anwendungen einer neuentwickelten Fluoreszenzfluktuationsmethode. Dissertation at the University of Basel, Switzerland.

Nicoli, D. F., J. Briggs, and V. B. Elings. 1980. Fluorescence immunoassay based on long time correlations of number fluctuations. *Proc. Natl. Acad. Sci. USA.* 77:4904–4980.

Palmer, A. G., and N. L. Thompson. 1987*a*. Theory of sample translation in fluorescence correlation spectroscopy. *Biophys. J.* 51:339–343.

Palmer, A. G., and N. L. Thompson. 1987*b*. Molecular aggregation characterized by high order autocorrelation spectroscopy. *Biophys. J.* 52:257–270.

Peters, R., J. Peters, K. H. Tews, and W. Bahr. 1974. A microfluorometric study of translational diffusion in erythrocyte membranes. *Biophys. Acta.* 367:282–294.

Petersen, N. O. 1984. Diffusion and aggregation in biological membranes. *Can. J. Biochem. Cell. Biol.* 62:1158–1166.

Petersen, N. O. 1986*a*. Scanning fluorescence correlation spectroscopy. I. Theory and simulation of aggregation measurements. *Biophys. J.* 49:809–816.

Petersen, N. O. 1986*b*. Scanning fluorescence correlation spectroscopy, II. Application to virus glycoprotein aggregation. *Biophys. J.* 49:817–820.

Petersen, N. O., and E. L. Elson. 1986. Measurements of diffusion and chemical kinetics by fluorescence photobleaching recovery and fluorescence correlation spectroscopy. *Methods Enzymol.* 130:454–484.

Schindler, H., and J. P. Rosenbusch. 1978. Matrix protein from Escherichia Coli outer membrane forms voltage dependent channels in lipid bilayers. *Proc. Natl. Acad. Sci. USA.* 75:3751–3755.

Schindler, H., and J. P. Rosenbusch. 1981. Matrix protein in planar membranes: cluster of channels in a native environment and their functional reassembly. *Proc. Natl. Acad. Sci. USA.* 78:2302–2306.

Wagner, M. L., and H. A. Scheraga. 1956. Gouy diffusion studies of serum albumin. *J. Phys. Chem.* 60:1066–1076.

Weissman, M., H. Schindler, and G. Feher. 1976. Determination of molecular weights by fluctuation spectroscopy: application to DNA. *Proc. Natl. Acad. Sci. USA.* 73:2776–2780.

Wilschut, J., N. Duzgunes, and D. Papahadjopolous. 1981. Calcium/magnesium specificity in membrane fusion: kinetics of aggregation and fusion of phosphatidylserine vesicles and the role of bilayer curvature. *Biochemistry.* 20:3126–3133.